Thermochimica Acta 707 (2022) 179096

Contents lists available at ScienceDirect

Thermochimica Acta

journal homepage: www.elsevier.com/locate/tca

The influence of calcium lignosulphonate addition on non-isothermal pyrolysis and gasification of demineralised bituminous coal fines

R.C. Uwaoma [a,*], M.P. Seheri [b], C.A. Strydom [a,b], J.R. Bunt [a], R.H. Matjie [a]

[a] Centre of Excellence in Carbon-based Fuels, North-West University, Potchefstroom Campus, Private Bag X6001, Potchefstroom 2520, South-Africa
[b] School of Physical and Chemical Sciences, North-West University, Potchefstroom Campus, Private Bag X6001, Potchefstroom 2520, South Africa

ARTICLE INFO

Keywords:
Demineralised coal fines
Calcium lignosulphonate
Pyrolysis
Gasification

ABSTRACTS

Amorphous calcium lignosulphonate (CaLS), a by-product of the paper industry, was evaluated as an adhesive to bind demineralised bituminous coal fines in various weight percentage ratios. Sequential acid (HCl, HF, HCl) leaching was used to reduce mineral matter content in the coal fines. The pyrolysis and gasification of the samples were investigated in laboratory-scale experiments to determine the effect of the CaLS addition on the pyrolysis and gasification reactivities. Coal-CaLS blends consisting of 5, 10, and 15% calcium lignosulphonate were prepared, compressed into pellets, and characterised using proximate, X-ray diffraction, and X-ray fluorescence analyses. An increase in binder concentration increases the mechanical strength of the pellets due to the increased interparticle contact area. The relative coal gasification reaction reactivity ($1/T_{max}$ and $0.5/T_{50}$), which was determined from the derivative thermogravimetry curves, increases with CaLS addition. The experimental results revealed that these wastes (coal fines and calcium lignosulphonate) could be utilised in thermochemical processes. Utilising these wastes will reduce the environmentally unfriendly volumes of amorphous calcium lignosulphonate and coal fines particles.

1. Introduction

Coal utilisation plays a significant role in the global- and local economies. Due to South Africa's large coal reserves and growing population, coal will continue contributing to energy production. Over 90% of South Africa's energy needs are met by coal-fired processes [1]. However, due to intensive mining activities such as processing and handling coal, which includes washing, screening, and crushing to satisfy basic energy needs, coal fines are produced, discarded into slimes dams, drinking water sources, and old underground workings [2,3].

The coal fines, which are regarded as waste, pose serious threats to the environment, including acid mine drainage, spontaneous combustion risk, explosion, and the disadvantage of adding more waste to the environment [2,3]. Apart from problems associated with transportation, processing, recovery, and tailings disposal, coal fines possess good thermal processing potential [2,4,5,6]. Coal fines are classified as low-grade coals as a result of their high mineral matter content. The utilisation of coal fines may improve South Africa's energy situation and limit coal mine waste deposits.

Research is ongoing regarding the utilisation of coal fines. Beneficiation of coal fines either by demineralisation or density separation and possible utilisation in coal conversion processes has proven to have the potential [7,8]. Lump coal is required for various industrial applications [2,5]. Pelletisation of coal fines is a process where fine particles can be transformed into mechanically strong agglomerates with good calorific value, producing a valuable fuel for domestic and industrial utilisation [5,9].

Pyrolysis is a thermal process used to degrade organic matter to yield pyrolytic products such as char, tar, pyrolytic water, and gases. Gasification is the chemical reaction of solid organic carbonaceous compounds in CO_2 or steam to produce mainly CO and H_2. These two thermal processes are important steps in the transformation of coal into useful products. Various factors have been identified to critically impact product distribution and reactivity during pyrolysis and gasification processes. These factors include composition, heating rate, particle size, and temperature.

Coal fines can be repurposed with the use of binders as agglomerating agents. Lignosulphonate, in either calcium or sodium forms, is known to have certain properties such as binding, dispersing, blending, and complexing [10]. In this study, calcium lignosulphonate (CaLS), a waste product in the paper industry, will be used as an agglomerating agent to bind coal fines and demineralised coal fines. CaLS have become

* Corresponding author.
E-mail address: 25452622@nwu.ac.za (R.C. Uwaoma).

https://doi.org/10.1016/j.tca.2021.179096
Received 11 April 2021; Received in revised form 30 August 2021; Accepted 3 November 2021
Available online 9 November 2021

easily accessible due to their production as waste material in the pulp and paper industry [10].

The application of calcium lignosulphonate as an agglomerant has been reported by Strydom et al. [5] and Leokaoke et al. [2]. Their studies showed that the blended pellets have adequate compressive strength to be used in industrial applications.

Ca-based additives can influence product distribution and reactivity during pyrolysis and gasification [11]. Calcium is classified as an essential alkaline earth metallic element that exhibits catalytic activity; however, its reaction with clay minerals in coal is lower when compared to other alkaline earth metallic elements, and they hardly devolatilised during thermal treatment. Various researchers have shown that Ca salts are a better choice for catalytic gasification than other alkaline salts [12–14].

A study carried out by Walker [12] on the gasification reactivity of calcium-loaded coal in air, CO_2, and steam showed that coal samples with added calcium demonstrated improved reactivity in gasification atmospheres compared to the samples without Ca-loading. Similarly, Murakami et al. [14], in their study, on the catalytic gasification of coal, compared two Ca-salts in their investigation ($CaCO_3$ and $Ca(OH)_2$), and results from their research show that $CaCO_3$ had a better catalytic performance as compared to $Ca(OH)_2$. Shuai et al. [13] also reported that $CaCO_3$ has proven to be a good catalyst. There is no literature on the pyrolysis and gasification of calcium lignosulphonate.

Increased production of coal fines remains a growing concern in South Africa. The blending of two undesirable waste products (South African coal fines and South African calcium lignosulphonate) has not been investigated in the past. This paper aims to indicate the effect of calcium-based lignosulphonate waste during pyrolysis and gasification of South African coal fines and demineralised samples of these coal fines. These samples and their derived char samples were submitted for proximate analyses, thermogravimetric analysis (TGA), and X-ray diffraction (XRD), and X-ray fluorescence (XRF) analyses.

2. Experimental procedure

2.1. Coal sample and demineralisation

A medium Rank-C bituminous coal sample from the South African Highveld was obtained using the international organisation for standardisation (ISO) standard methods, ISO 1988:1975 and ISO13909-4:2016 for sampling procedures. The coal sample was pulverised to −300 μm particle sizes and immediately sealed to avoid the samples' possible oxidation. The coal was demineralised using a sequential acid leaching method described previously [15]. Koening et al. [16]; Strydom et al. [17] stated in their study that HCl assisted in the decomposition of carbonates minerals in coal. HF dissolves most of the coal mineral matter (inherent mineral matter and extraneous minerals), including quartz and alumino-silicates [18,19].

The coal sample (80 g) was leached with 320 ml of a 10.2 M HCl solution for 24 h. The resulting solution was filtered and washed using a vacuum pressurized Buchner funnel. The residual sample was then leached with 320 ml of a 22.6 M HF solution for 24 h to dissolve mineral matter insoluble in HCl. The resulting slurry was again filtered and washed using a vacuum pressurised polypropylene Buchner funnel. The treatment final stage involves the leaching of resulting residues with 320 ml of 10.2 M HCl for 24 h. The residual product from the final stage of the acid treatment is regarded as the demineralised coal fines and is vacuum filtered and washed with distilled water. The washing process was continued until no evidence of acid was observed in the samples using a pH metre. The final product was left to dry in the oven at 80 °C. The acid treatment procedures were conducted at ambient temperature, and the demineralised coal fines samples were stored in a nitrogen pressurised desiccator. The efficiency of the demineralisation, E_d, was quantified using the following formula:

$$E_d = \left\{ \frac{A_o - A_d}{A_o} \right\} \times 100 \quad (1)$$

where A_o denotes the% ash yield of the coal fines before demineralisation and A_d is the% ash yield of the demineralised residue (wt.%, db).

2.2. Sample preparation

Mechanical size reduction and sieving following the ISO 1988:1975 and ISO13909-4:2016 sampling procedures were used to obtain the required sizes of the particles. Calcium lignosulphonate, received from a South African local pulping company, was used as a binder and sieved to the desired size. The coals and additives were mixed using a mortar and pestle and an electric mixer.

2.3. Pellet preparation

Coal-binder samples with loadings of 0 wt.%, 5 wt.%, 10 wt.%, 15 wt.% calcium lignosulphonate and 5 wt.% $CaCO_3$ were prepared using both the coal fines and the demineralised coal fines. The coal-binder mixtures were then pressed using an LRX Plus tensile test machine (Ametek Lloyd Instruments). Approximately 1 g of a mixture was loaded into a cylindrical die set with 13 mm internal diameter. The mixture was compressed using a force of 4000 N and a pressing rate of 10 mm/min. The samples were kept at the maximum pressure reached for 10 s. The pressed pellets were cured at 100 °C in an oven for a 24 h period and then stored in a closed container before testing the compressive strengths. This procedure was utilised to prevent the samples from oxidisation prior to analysis.

2.4. Tube furnace char preparation

A scrubbing system fitted with glass bottle scrubbers was connected to a high-temperature Elite thermal system TSH 12/75/610–2416CG+2116 O/T tube furnace. 25 g of the prepared samples (one parent coal fines sample, one demineralised coal fines sample, demineralised coal fines with 5%. wt., 10%. wt. and 15 wt.% of CaLS, with and without 5% $CaCO_3$) were weighed in a boat crucible. 100 mL of 1 M KOH scrubber solutions absorb the gases emitted during thermal treatment. The nitrogen flow through the tube was 100 mL/min. The program was set to a heating rate of 10 °C/min from ambient temperature up to a maximum temperature of 1000 °C. Once the maximum temperature was reached, the samples were allowed to cool to room temperature under nitrogen. The mass loss as a function of temperature was recorded. All samples were subjected to the same experimental conditions, and multiple runs were performed to ensure repeatability. The chars produced were further screened to −212 μm and submitted for the proximate, XRD, and XRF analyses. From henceforth the samples will be reconganised as: Coal fines (CF-0%); Coal fines char (CFC-0%); Coal fines + 5% CaLs (CF-5%); demineralised coal fines (DCF-0%); demineralised coal fine char (DCFC-0%); demineralised coal fines + 5% CaLs (DCF-5%); demineralised coal fines + 10% CaLs (DCF-10%); demineralised coal fines + 15% CaLs (DCF-15%); demineralised coal fine char + 5% CaLs (DCFC-5%); demineralised coal fine char + 10% CaLs (DCFC-10%); demineralised coal fine char + 15% CaLs (DCFC-15%).

2.5. Pyrolysis and gasification experiments

Thermogravimetric (TG) studies of the coal fines, demineralised coal fines, and blends of the demineralised coal fines and CaLS were conducted using a TA Instruments SDT-Q600 thermogravimetric analyser. 15 mg each of the samples was loaded in alumina pans. To ensure the TG chamber was inert prior to the pyrolysis experiment, the section was flushed with nitrogen gas (purity 99.9%) for 10 min. The temperature

Table 1
Proximate analysis, demineralisation efficiency, and gross calorific value results of the coal fines and demineralised coal samples with different percentages CaLS and $CaCO_3$ additions.

Sample identification	A	B	C	D	E	F	J	H	I	J
Inherent moisture (%)	6.1	1.7	6.1	4.8	4.6	3.1	2.8	3.2	2.8	3.1
Ash content (%)	27.4	37.4	29.3	40.6	1.1	1.6	3.2	4.2	4.6	3.5
Volatile Matter (%)	25.5	1.1	28.7	2.7	30.1	0.8	2.4	1.6	1.7	1.1
Fixed carbon (%)	41	59.8	35.9	51.9	64.2	94.5	91.6	91	90.9	92.3
E_d (%)	96	95.7	–	–	–	–	–	–	–	–
Gross calorific value (MJ/kg)	19.5	–	18.2	–	28.5	–	27.6	26.2	26.8	27.1

E_d- Effectiveness of demineralization; A= CF; B= CFC; C = CF-15%; DCFC- 15%; *E*= DCF-0%; *F*= DCFC-0%; *G*= DCFC-5%; *H*= DCFC-10%; *I*= DCFC-15%; *J*= DCFC- 5% $CaCO_3$.

was allowed to stabilise at room temperature. The samples' pyrolysis was conducted by heating the samples from ambient temperature to 900 °C at a flow rate of 10 °C min^{-1}. A continuous flow of 75 mL min^{-1} nitrogen gas was used during the pyrolysis experiments. The samples were then allowed to cool down (in situ) to room temperature under the nitrogen atmosphere, to prevent the sample from oxidising.

After cooling the samples to ambient temperature, the atmosphere was switched to CO_2 (purity 99.9%). The samples were heated under CO_2 from ambient temperature to 1200 °C at a specified rate and a CO_2 flow rate of 20 ml min^{-1}. CO_2 non-isothermal reaction conditions were used in this investigation, using Heating rates of 5,10, 15, and 20 °C min^{-1} were used.

To quantitatively characterise the reactivities of the samples, the following properties were used: initial weight loss temperature T_i, maximum conversion rate temperature T_m, and total weight loss temperature T_f. These values were estimated using methods reported elsewhere [20,21]. These parameters were used to calculate the gasification index S, given in Eq. (2) [22].

$$S = \frac{(dx/dt)_{max} \cdot (dx/dt)_{mean}}{T_i^2 \cdot T_f} \quad (2)$$

where $(dx/dt)_{max}$ is the maximum rate at which the gasification occurs and $(dx/dt)_{mean}$ gives the mean value of the gasification rate.

Conversion (X) at each value of mass at a time (t) from the non-isothermal gasification experiments was calculated using Eq. (3). Initial char weight is indicated by (m_0) and final weight of the sample after gasification is referred to as (m_f). The char weight at time (t) is indicated by (m_t). Eq. (4) was used to calculate the gasification rate (r), while Eq. (5) was used to calculate the reactivity index at 50% conversion.

$$X = \frac{m_0 - m_t}{m_0 - m_f} \quad (3)$$

$$R_{50} = \frac{0.5}{\tau_{50}} \quad (4)$$

2.6. Proximate analysis

Proximate analysis of the coal fines, demineralised coal sample, and blends and their char samples was conducted following the ISO 17,246:2010 standard at the laboratory of Bureau Veritas Testing and Inspections SA (Pty) Ltd., Pretoria. A U-Therm FC-TGA-D automatic proximate analyser was used.

2.7. XRD and XRF analyses

XRD analysis was conducted to qualify and quantify the proportions of crystalline and amorphous phases in the samples [23,24]. The samples were subjected to mineralogical analysis using an X'Pert PRO PANalytical (Philips)– Unit 2 XRD instrument with anode material cobalt and Rietveld-based X'Pert HighScore Plus software. The samples were first spiked with 20% Si.

The samples were also characterised by XRF analysis to determine the concentrations of inorganic elements present in the ash [25]. The ashed samples were fused into borosilicate discs and analysed using a PANalytical (Axios Max) WD-XRF spectrometer equipped with a 50 kV Rh-anode X-ray tube six filters, a P10 gas purge facility, and a high-resolution silicon drift detector.

3. Results and discussion

3.1. Proximate analysis

The proximate analysis results determined on an air-dried basis are presented in Table 1. The coal fines sample has a relatively high percentage ash yield of 27.4 wt.% with low fixed carbon content (41.0 wt.%) with the ash yield comparable to reported data for South African coal fines [9,26]. The ash yield for the demineralised coal sample is 1.1 wt.%, indicating effective removal of almost all of the aluminosilicate and minerals present in the waste coal. Table 1 also shows that the demineralisation efficiency of the demineralised coal samples and its derived

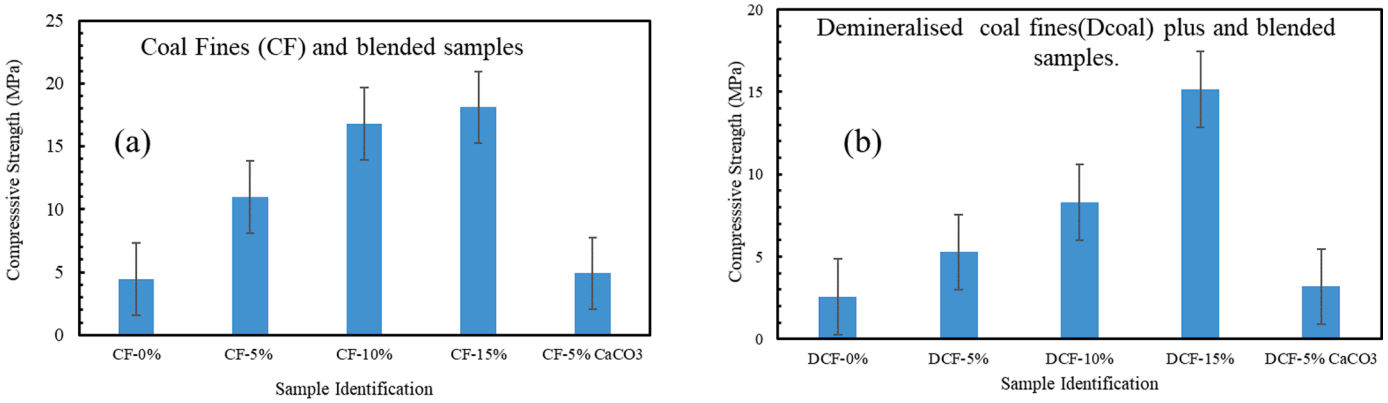

Fig. 1. Compressive strength values of the (a) coal fines and (b) demineralised coal fines samples and their different blends.

Table 2
XRD analysis results of coal fines and demineralised coal samples with different CaLS loading (wt.%, gfb).

	Sample names									
Mineral	A	B	C	D	E	F	G	H	I	J
Quartz	4.3	17.3	3.6	16.8	–	–	–	–	–	–
Kaolinite	14.6	0.0	12.2	0.0	–	–	–	–	–	–
Calcite	0.1	0.0	0.2	0.0	–	–	1.3	1.7	2.8	3.8
Muscovite	1.6	0.7	0.8	2.4	–	–	–	–	–	–
Microcline	–	0.3	–	0.3	–	–	–	–	–	–
Anatase	–	0.2	–	0.5	–	–	–	–	–	–
Rutile	–	0.1	–	0.1	–	–	–	–	–	–
Graphite	–	0.9	–	0.7	–	–	–	–	–	–
Anorthite	0.0	7.2	–	8.1	–	–	–	–	–	–
Mullite	0.0	2.6	0.0	1.4	–	–	–	–	–	–
Gypsum	0.3	0.4	0.6	0.5	–	–	–	–	–	–
Bassanite	–	0.3	–	0.0	–	–	–	–	–	–
Anhydrite	–	0.6	–	1.2	–	–	–	–	–	–
Oldhamite	–	2.3	–	3.0	–	–	0.5	0.7	1.2	1.8
Pyrite	–	0.4	–	0.1	0.8	1.3	–	–	–	–
Magnetite	–	0.6	–	0.6			–	–	–	–
Pyrrhotite	0.1	0.7	0.2	1.1	–	–	–	–	–	–
Haematite	–	0.2	–	0.3	–	–	0.8	0.5	0.7	0.8
cristobalite	–	0.5	–	0.3	–	–	–	–	–	–
Portlandite	–	0.1	–	0.1	–	–	–	–	–	–
Amorphous	75.6	64.6	78.0	62.5	99.1	98.7	97.5	97.2	95.3	93.8

-Not determined.
A= CF-0%; B= CFC-0%; C= CF-15%; D = CFC-15%; *E*= DCFC-0%; *F*= DCFC-5%; *G*= DCFC-10%; *H*= DCFC-15%; *I*= DCFC- 5% $CaCO_3$.

chare was 96%.

Table 1 shows that after demineralisation, the volatile matter and fixed carbon contents of the demineralised coal sample increased compared to those of the untreated coal fine samples due to the substantial reduction in the ash yield of the demineralised sample.

Pyrolysis of the demineralised coal fines causes a reduction in the volatile matter content, while the fixed carbon content increased as expected. The char samples of the demineralised CaLS blends (5,10, and 15 wt.%) show a slight increase in ash yield and a decrease in the fixed carbon contents as the percentages of CaLS increases in each sample.

The calorific value is significant to indicate energy efficiency [27]. The gross calorific value of the coal fines was 19.4 MJ/kg, and that of the demineralised coal fines 28.5 MJ/kg (Table 1). The higher calorific value of the demineralised coal fines is due to the higher fixed carbon and volatile matter contents (64.2 and 30.1 wt.% a.d.b, respectively). Coal fines have lower fixed carbon and volatile matter contents (41.0 and 25.5 wt.% a.d.b, respectively). Slight decreases in the calorific values were observed for the samples with calcium lignosulphonate (CaLS) additions.

3.2. Compressive strength

The mechanical strength of the coal fines, demineralised coal, and their blends were evaluated. The coal fines, demineralised coal, and blended samples were pelletised and left to dry overnight in an oven at 100 °C temperature. The compressive strength test values determined as described are summarised in Fig. 1. The demineralised and blended samples showed lower compressive strengths than those of the coal fines and its blended samples. The higher compressive strength of the coal fines was attributed to the aluminosilicate and fluxing elements present in the coal fines, which helped harden the produced pellets and thus increased the strengths. Fig. 1 shows that the compressive strength values increased with increasing CaLS addition (5, 10, and 15 wt.%) for untreated coal fines and demineralised coal fines samples. $CaCO_3$ addition does not significantly increase the compressive strength values of the coal fines or the demineralised coal fines samples, implying that $CaCO_3$ is not acting as a binder.

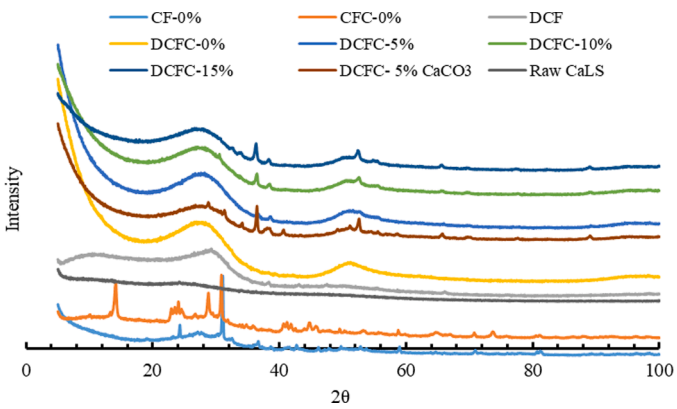

Fig. 2. X-ray diffractograms of coal fines, demineralised coal, and CaLS blended coal samples.

3.3. XRD analysis

The XRD analysis results of coal fines, calcium lignosulphonate (CaLS), and blends of coal fines and CaLS are given in Table 2 and Fig. 2. The crystalline part of the untreated coal fines samples consists mainly of kaolinite (14.6%), quartz (4.3%), and muscovite (1.6%) with minor proportions of gypsum (0.3%), calcite (0.1%), and pyrrhotite (0.1%). The presence of pyrrhotite in the coal fines was due to pyrite oxidation during the sample ageing and weathering. Mullite present in all chars resulted from the transformation of extraneous kaolinite at high temperatures or via crystallisation of mullite from calcium-alumina-silicate molten solution during the heating under nitrogen. Matjie et al. (2018) confirmed the presence of anorthite and mullite in the chars of South African coal and blends of coal and K_2CO_3 samples treated at elevated temperature of 900 °C under nitrogen and air conditions.

The XRD results of the thermally treated coal fines and amorphous CaLS (Table 2 and Fig. 2) show that these samples contain bassanite, gypsum, and anhydrite. The transformed product (CaO) of calcite can primarily react with SO_2 from pyrite oxidation at elevated temperatures to form anhydrite (Matjie et al., 2015). Organic Ca and organic sulphur in the samples Matjie et al. [28] can interact at < 600 °C to form bassanite, which transforms above 600 °C to anhydrite. The presence of

Table 3
XRF and alkaline index results of coal fines and demineralised coal samples with different CaLS loading (wt.%).

Elements	A	B	C	D	E	F	G	H	I	J
SiO_2	13.80	18.65	13.2	0.05	0.08	0.20	0.15	0.10	0.05	0.04
Al_2O_3	7.76	9.96	7.6	0.13	0.19	0.15	0.18	0.17	0.10	0.01
TiO_2	0.37	0.54	7.2	0.18	0.27	0.21	0.26	0.25	0.26	0.00
Fe_2O_3	1.22	1.69	5.1	0.27	0.38	1.36	1.42	1.50	0.33	0.02
CaO	1.32	1.90	0.7	0.03	0.04	1.00	1.60	2.00	3.00	7.25
MgO	0.70	0.85	0.5	0.02	0.04	0.07	0.08	0.08	0.06	0.21
Na_2O	0.15	0.20	0.26	0.00	0.00	0.05	0.01	0.01	0.05	0.00
K_2O	0.26	0.51	0.2	0.00	0.00	0.05	0.08	0.03	0.03	0.11
MnO	0.02	0.03	0.1	0.00	0.00	0.00	0.01	0.02	0.00	0.05
Ash content	25.59	34.34	34.86	0.67	1.01	3.08	3.77	4.15	3.88	7.68
Moisture	4.76	4.55	5.20	3.85	7.54	7.21	7.16	7.12	6.49	8.09
LOI	69.27	60.20	70.34	95.23	91.18	90.25	90.00	88.23	87.33	84.20
SiO_2 +Al_2O_3 +TiO_2 (A)	21.93	29.15	28.00	0.35	0.54	0.56	0.58	0.51	0.42	
Fe_2O_3 + CaO + MgO + Na_2O + K_2O (B)	3.64	5.16	6.76	0.32	0.46	2.52	3.18	3.62	3.47	
B/A	0.17	0.18	0.24	0.93	0.85	4.48	5.46	7.04	8.30	
B/A X ash content	4.25	6.08	8.42	0.62	0.86	13.82	20.57	29.20	32.24	

A= CF-0%; B= CFC-0%; C = CFC-15%; *D*= DCF-0%; *E*= DCFC-0%; *F*= DCFC-5%; *G*= DCFC-10%; *H*= DCFC-15%; *I*= DCFC-5% $CaCO_3$; *J*=Raw CaLS.

bassanite and gypsum in the chars can be attributed to anhydrite's hygroscopic nature during cooling, storage, and analysis of these samples. XRD analysis also reveals that oldhamite is present in all samples treated at 1000 °C under nitrogen. At higher temperatures, oxygen concentration decreases sharply, which drives hydrogen sulphide (H_2S) formation Shirai et al. [29] and reduces calcite to oldhamite [28]. The amounts of calcium sulfate, produced through reactions of CaO (from calcite) and SO_2 (from the oxidation of pyrite), can be reduced in the presence of carbon or carbon monoxide by generating oldhamite at temperatures in the range of 950 - 1500 °C under inert atmospheres [30]. The bassanite, oldhamite, and anhydrite in the chars of the coal fines were not present in the original coal fines sample, amorphous calcium lignosulphonate, or pellets of these wastes.

As expected, the demineralised samples have a small proportion of pyrite present with a significant fraction of amorphous carbon. The increase in amorphous phase percentages in the demineralised coal sample compared to the coal fines sample is mainly ascribed to the mineral matter removal by the acid leaching process, leading to an increase in the volatile matter and fixed carbon percentages. The XRD results for the coal fines and the demineralised coal samples clearly show the effective removal of most of the crystalline mineral phase.

The X-ray diffractograms of the coal fines, demineralised coal fines, and their blends are presented in Fig. 2. It can be observed that the coal fines and its char show a peak at 26.64° and 30.38° (small peaks at 2θ = 31.25°), which are assigned to the presence of SiO_2 in coal. This peak was seen to be pronounced after pyrolysis treatment. The diffractograms of the coal fines and the demineralised sample show that the mineral peaks (kaolinite and quartz) present in the coal fines sample disappear after the acid treatment.

The demineralised coal char with CaLS blends showed a small peak at 2θ = 38.25° This peak increases with a corresponding increase in CaLS addition (5,10,15 wt.%). The peak in this region is attributed to CaS and traces of haematite (which may overlap with pyrite), fluorite and calcite minerals in the calcium lignosulphonate blends.

3.4. XRF analysis

The XRF analysis was performed to determine the elemental composition of the coal ash (Table 3). The ash of the coal fines was mostly Si, Al, Fe, and Ca presented in their oxide forms of SiO_2, Al_2O_3, Fe_2O_3, and CaO. For the demineralised coal sample, the inorganic compounds are present in extremely low concentrations (< 0.4 wt.% on an LOI basis), and these were Al_2O_3, TiO_2, and Fe_2O_3. After demineralisation, the concentrations of minerals are greatly reduced, as expected. As stated in previous study findings, acid leaching is useful in decomposing extraneous minerals, such as aluminium silicate

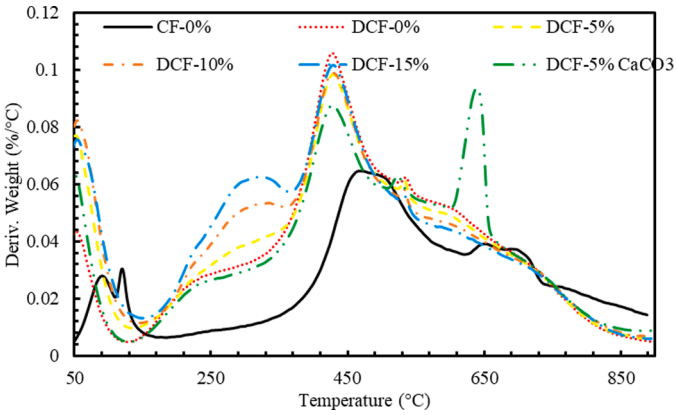

Fig. 3. DTG curves of coal fines, demineralised coal fines, and its additives during pyrolysis.

compounds, pyrite, and carbonates in the coal [31–33].

$$AI_1 = Ash\ yield\ (\%) * \frac{Fe_2O_3 + CaO + MgO + Na_2O + K_2O}{SiO_2 + Al_2O_3 + P_2O_5} \quad (5)$$

The addition of calcium lignosulphonate to the demineralised coal slightly increases CaO concentration in the blended samples. As expected, the addition of $CaCO_3$ to the demineralised sample resulted in the highest CaO concentration, with a higher percentage of calcite also observed in this sample (Table 2). Alkali index (AI) was evaluated using Equation 5; results obtained from the AI are summarised in Table 3. The base to acid ratios, which give the alkali indices, ranged from 0.62 to 32.24. The blended samples showed higher base to acid ratios, which may affect the gasification reactivities of these samples.

3.5. Pyrolysis of samples

The DTG and the mass loss curves obtained during the pyrolysis of the samples are presented in Figs. 3-5. Coal fines showed three distinctive DTG peaks under an inert atmosphere (pyrolysis). The peaks found between 100 and 200 °C are ascribed to the loss of inherent moisture in the samples. The peaks in the range of 350–550 °C can be linked to the loss of light aliphatic components from light organic species in the coal [34]. The peak in the 550–800 °C region is ascribed to the transformation of minerals (clays, carbonates, sulfides) present in the coal chars. The demineralised coal fines sample showed only two peaks during pyrolysis; the inherent moisture peak (100–200 °C) and the peak at which volatiles was liberated (350–550 °C). No DTG peak associated

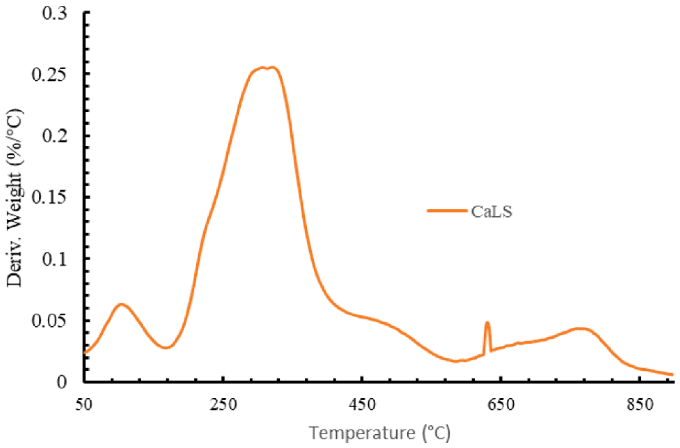

Fig. 4. DTG curve of CaLS.

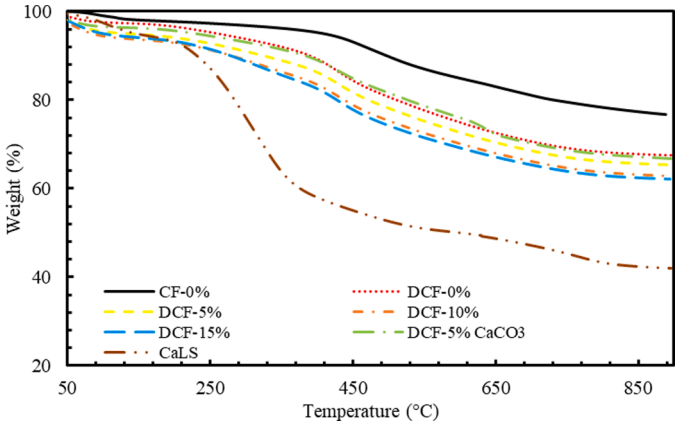

Fig. 5. Mass loss curves for the coal fines, demineralised coal, and blended samples.

with the mineral transformation (550–800 °C) was observed for the demineralised sample, as expected.

The calcium lignosulphonate sample showed three DTG peaks (Fig. 4). The first peak between 50 and 200 °C can be accredited to the loss of inherent moisture from lignin [35,36]. A second peak observed in the range of 170–450 °C is due to lignin degradation, and this is also the pyrolysis zone, giving the largest response. In this zone, the higher molecular mass components present in the CaLS and lignin are degraded, which leads to volatiles being released. A mass loss of approximately 20% was observed at the final temperature of 900 °C. The third very small DTG peak is due to the decomposition and transformation of minerals in the amorphous calcium lignosulphonate samples. The demineralised coal and 5, 10, and 15 wt.% calcium lignosulphonate and 5% $CaCO_3$, blended samples show large peaks between 250 and 350 °C, with a shoulder onto the next peak at 450 °C. This shoulder, which increases with increasing CaLS content in the blended sample, is attributed to lignin degradation. According to Liodakis et al. [37], calcium carbonate compounds are likely to decompose into CaO and CO_2 in the temperature range between 600 and 750 °C with a DTG peak, usually at 700 °C.

The mass loss curves of the coal fines, demineralised coal fines, and blended samples are shown in Fig. 5. As expected, the mass loss percentages at 900 °C for the coal fines were observed to be higher than those of the demineralised samples. The demineralised samples and the samples with CaLS addition showed lower mass losses than those of the coal fines, which increases as the ratio of the CaLS in the blends increases.

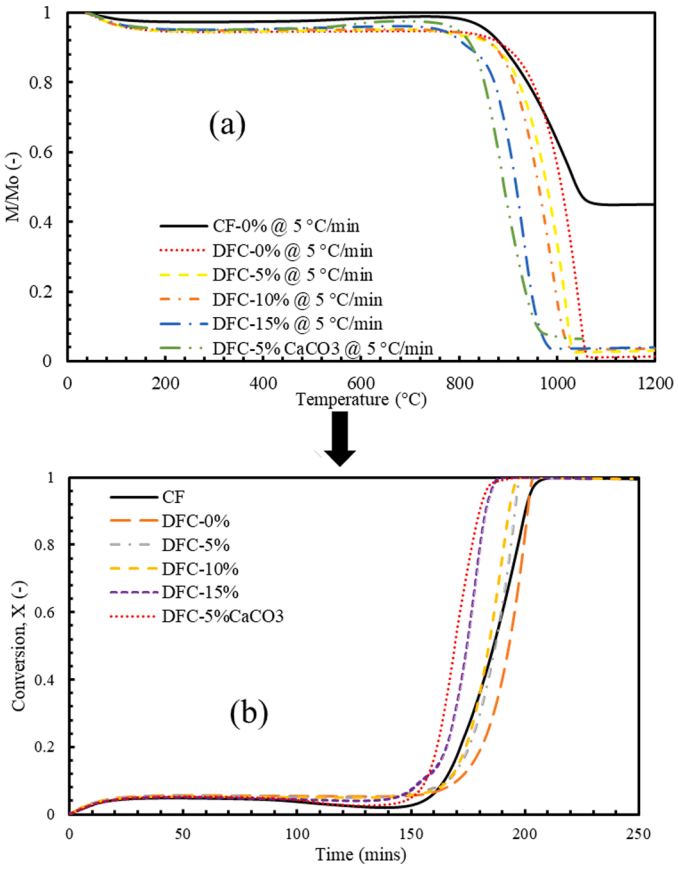

Fig. 6. (a)Relative mass loss (TG) (b) conversion curves of the chars derived from the demineralised coal and blended samples in a CO_2 atmosphere.

The mass loss percentages of the samples at 900 °C were found to be 23.3, 58.0, 32.5, 33.7, 34.6, 37.2, and 37.9% for coal fines, calcium lignosulphonate (CaLS), demineralised coal fines, DC-5% $CaCO_3$, DCF-5%, DCF-10%, DCF-15% respectively. The mass losses are consistent with the volatile matter results, as summarised in Table 1.

3.6. Gasification of samples

Thermogravimetric mass loss curves and conversion curves of samples in a CO_2 atmosphere are presented in Fig. 6 (a, b). The mass loss data in Fig. 6a obtained during the experiment were converted in Fig. 6b using the conversion Eq. (3). These curves represent the samples'

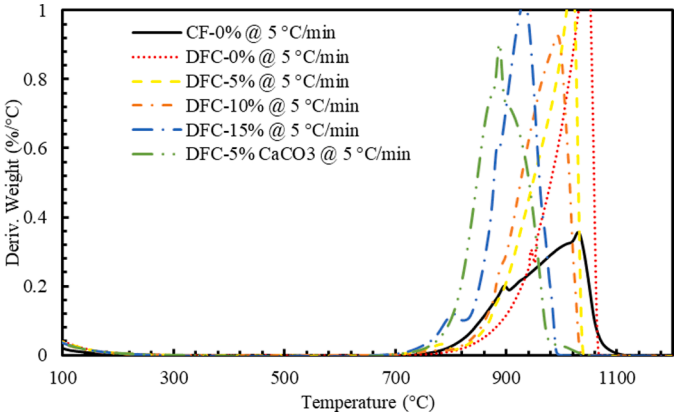

Fig. 7. DTG curves of the chars derived from the demineralised coal and blended samples in a CO_2 atmosphere.

Table 4
Temperatures at initial mass loss (T_i), termination mass loss (T_f) and maximum rate of mass loss (T_{max}).

Sample ID	T_i (°C)	T_{max} (°C)	T_f (°C)	$\Delta T(T_f - T_i)$ (°C)	$1/T_{max}$ (°C^{-1}) X10^4	S X 10^{12}	dx/dt_{max} (min^{-1})	dx/dt_{mean} (min^{-1})	t_{50} (min)	$0.5/t_{50}$ (min^{-1})
Coal fines										
CF-0%	771	1032	1120	349	9.69	0.197	0.033	0.0040	186.2	0.0027
Dcoal + additives										
DCF-0%	834	1100	1150	316	9.09	0.341	0.062	0.0041	192.9	0.0026
DCF-5%	789	1019	1050	261	9.81	0.416	0.063	0.0043	170.3	0.0029
DCF-10%	732	974	1033	301	10.27	0.441	0.065	0.0043	154	0.0032
DCF-15%	735	938	950	215	10.66	0.501	0.068	0.0047	140	0.0036
DCF-5% $CaCO_3$	749	850	970	221	11.76	0.461	0.051	0.0050	125	0.0040

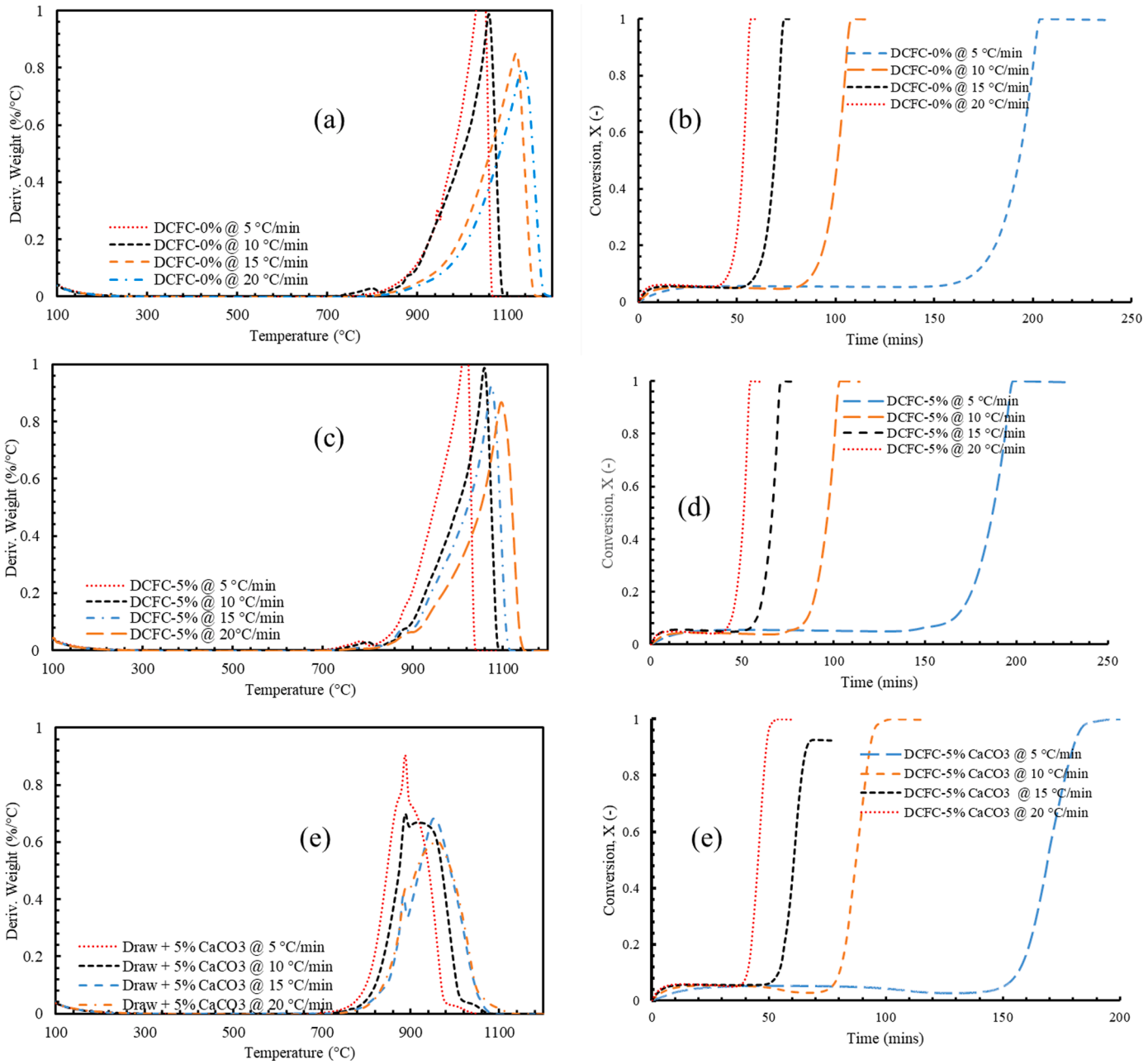

Fig. 8. Gasification mass loss and DTG curves using different heating rates: (a) DCFC-0% (DTG curve); (b) DCFC-0% (conversion curve); (c DCFC-5% (DTG curve); (d) DCFC-5% (conversion curve); (e) DCFC-5% $CaCO_3$ (DTG curve), (f) DCFC-5% $CaCO_3$-char (conversion curve).

Table 5
Characteristic gasification parameters of demineralised coal samples with different CaLS loading chars at four different heating rates.

Char	Heating rate (°C min^{-1})	T_i (°C)	T_{max}(℃)	T_f (℃)	dx/dt_{max} (min^{-1})	dx/dt_{mean} (min^{-1})	S X 10^{12}	$1/T_{max}$ ($^{-}$℃)	t_{50} (min)	$0.5/t_{50}$ (min^{-1})
DCFC-0%	5	834	1048	1079	0.062	0.00414	0.34	0.00095	192.9	0.0025
	10	848	1097	1151	0.093	0.00870	1.00	0.00091	100.9	0.0050
	15	859	1124	1181	0.134	0.01309	2.02	0.00089	68.9	0.0072
	20	881	1140	1213	0.167	0.01664	3.00	0.00088	53.1	0.0094
DCFC-5%	5	789	1019	1056	0.063	0.00432	0.42	0.00098	170.3	0.0029
	10	835	1062	1108	0.106	0.00874	1.20	0.00094	96.8	0.0052
	15	843	1077	1132	0.146	0.01302	2.40	0.00093	66.4	0.0075
	20	851	1101	1162	0.178	0.01675	3.30	0.00091	50.8	0.0010
DCFC- 5% $CaCO_3$	5	749	888	986	0.068	0.00497	0.46	0.00113	125	0.0040
	10	773	922	1059	0.126	0.00919	1.40	0.00108	87.3	0.0060
	15	794	959	1092	0.153	0.01326	2.41	0.00104	60.7	0.0082
	20	816	967	1110	0.170	0.01690	3.45	0.00103	45.4	0.0110

behaviour during gasification. Fig. 6 shows no substantial mass loss at temperatures below 750 °C for all the samples. These findings indicate that gasification reactions start taking place at temperatures above 750 °C [38].

The coal fines and demineralised coal reached a total mass loss at the final temperature of 1100 ^{O}C of 36% and 1%, respectively. The mass loss behaviour did not differ significantly during the CO2 heat treatment for the demineralised coal fines and blended demineralised coal and calcium lignosulphonate samples. The demineralised coal sample showed a much larger mass loss when compared to coal fines, consistent with the proximate analysis results in Table 1 and the ash yields. The gasification mass loss curves of the demineralised and blended samples show that the samples mainly consist of carbon, with a very small percentage of inorganic, as indicated in the proximate analysis and XRD results Tables 1 and 2.

The DTG curve of samples in a CO_2 atmosphere is presented in Fig. 7. The DTG curves are used to identify characteristic reactivity temperatures. The temperatures are identified as: the temperature at which the gasification process started (T_i), the temperature at which the highest rate of mass loss occurs (T_{max}), and the temperature where the mass loss is concluded (T_f) [20–22]. The coal fines DTG curve was shown to be broader, while the demineralised coal and the blended samples' DTG curves were observed to be narrower.

Table 4 summarises the maximum rate of mass loss temperature (T_{max}) and the time needed for 50% mass loss per reaction per sample (t_{50}). The gasification reactivities ($1/T_{max}$) evaluated from T_{max} is also presented in Table 4. The $1/T_{max}$ values indicated that an increase in CaLS in the blends increases the gasification reactivities. The Ti temperatures of the chars showed the following increasing order of gasification onset (and thus reactivity): DCFC-5%$CaCO_3$<DCFC-15% < DCFC-10%< DCFC-5%< CFC-0%< DCFC-0%. T_{max}, as well as T_f of char samples, follow the same order. The 50% conversion of the DCFC-15% sample was recorded as the highest, followed by those of the DCFC-5% $CaCO_3$ and DCFC-10%.

The time to reach a 50% mass loss of the gasification reaction (or conversion of 0.5 for the gasification reaction) was also used to indicate the reactivity. Eqs. (2) and 4 were used to obtain reactivities tabled in Table 4. An increase in the amounts of CaLS in the blends (5, 10, and 15 wt.%) leads to increases in the reactivity values. The higher reactivity values for the coal fines char compared to the demineralised coal fines char sample are attributed to the mineral matter present in the coal fines char.

3.7. Gasification parameter (S)

Fig. 8 gives the mass loss curves at 4 different heating rates. The mass loss values at the different heating rates were used to determine the gasification parameters (S) as given in Eq. (2), and these are summarised in Table 5. The gasification index (S), dx/dt_{mean}, and dx/dt_{max} increased as heating rate increases. The demineralised coal fines were shown to have a lower gasification index and a higher t_{50} than those blended with CaLS at the different heating rates. This indicates that the Ca-containing minerals in the blends may aid in facilitating the gasification reaction process.

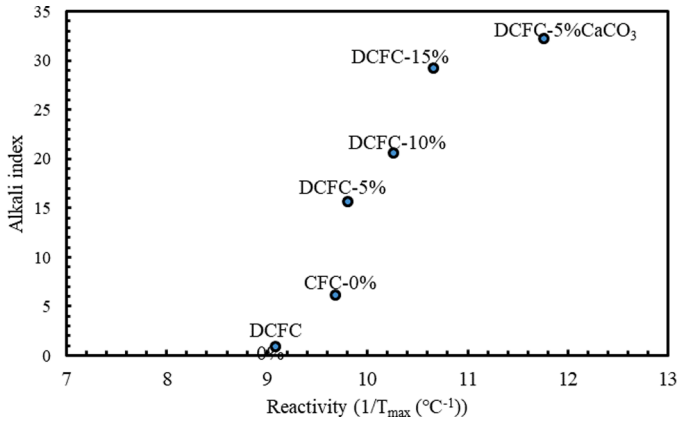

Fig. 9. Correlation between reactivity expressed at $1/T_{max}$ and alkaline indices of samples.

3.8. Correlation of alkali index and reactivities

Fig. 9 presents the correlation between the alkali indices and the gasification reactivity expressed as $1/T_{max}$ as previously described [39, 40]. Researchers have shown that alkali compounds containing potassium, sodium, and calcium play catalytic roles during gasification reactions. In their study, Zhang et al. [41] stated that potassium-containing compounds are the strongest gasification catalysts, followed by sodium and calcium compounds. A direct correlation between the samples' reactivities and their amounts of added CaLS in the blends was observed (Fig. 8). The char samples produced with the 5% $CaCO_3$ showed the highest reactivity, with the demineralised coal fines sample having the lowest reactivity. These reactivities increased with an increase in the CaLS blend ratio. The Ca present in the CaLS seems to act as a catalyst during the non-isothermal CO_2 reactivity tests. The increase in reactivity can be ascribed to the catalytic effect of the alkaline earth metal in the CaLs and the residual char from the additive (Fig. 5). As seen in Fig. 5 increase in additive loading leads to a decrease in the amount of char.

4. Conclusion

The compression strengths of the pellets of coal fines samples increases in blends with increasing CaLS percentages for both the

untreated and demineralised coal fines samples. The proximate analysis shows that the acid leaching resulted in a high dissolution efficiency of mineral matter by decreasing the ash yield from 27.4% to 1.1%. Thermogravimetric analysis results of the prepared coal char samples with CaLS and $CaCO_3$ indicate that the added compounds influenced CO_2 gasification reaction reactivity. The relative coal gasification reactivity, measured as $1/T_{max}$, with T_{max}, the temperature at a maximum rate of the reactions, increased with increasing CaLS loadings and for the char prepared from the 5% $CaCO_3$, addition. Experimental results obtained reveal that these wastes (coal fines and calcium lignosulphonate) may be utilised in thermochemical processes to decrease costs and volumes of amorphous calcium lignosulphonate and fine coal particles linked to transporting and disposing of these wastes.

Declaration of Competing Interest

On behalf of my colleagues, we declare there is no conflict of interest in the manuscript and declare our interest in publishing our original laboratory work in your reputable journal.

Acknowledgements

I thank the School of Physical and Chemical Science at North-West University and the SARChI chair in Coal Research (Grant no: 86880) for their financial support in carrying out this project. Dr. Sabine Verryn of Council for Geoscience Pretoria is thanked for her assistance with the XRF and XRD analyses. Bureau Veritas Testing and Inspections, South Africa, is thanked for their help with the proximate analysis. Opinions, findings, and conclusions or recommendations expressed in this publication generated by the NRF supported research are that of the authors alone. The NRF accepts no liability whatsoever in this regard.

References

[1] C. Arndt, R.Davies C, S. Gabriel, K. Makrelov, B. Merven, F. Hartley, J. Thurlow, A sequential approach to integrated energy modelling in South Africa, Appl. Energy. 161 (2016) 591–599.
[2] N.T. Leokaoke, J.R. Bunt, H.W. Neomagus, F.B. Waanders, C.A. Strydom, T. S. Mthombo, Manufacturing and testing of briquettes from inertinite-rich low-grade coal fines using various binders, J. South. Afr. Inst. Min. Metall. 118 (2018) 83–88.
[3] S.J. Mangena, V.M. Du Cann, Binderless briquetting of some selected South African prime coking, blend coking and weathered bituminous coals and the effect of coal properties on binderless briquetting, Int. J. Coal Geol. 71 (2007) 303–312.
[4] E. Muzenda, Potential uses of South African coal fines: a review, in: International Conference on Mechanical, Electronics and Mechatronics Engineering, 2014.
[5] C.A. Strydom, T.S. Mthombo, J.R. Bunt, H.W. Neomagus, Some physical and chemical characteristics of calcium lignosulphonate-bound coal fines, J. South. Afr. 118 (2018) 1277–1283.
[6] S. Mani, S. Sokhansanj, Bi.A.Turhollow X, Economics of producing fuel pellets from biomass, Appl Eng Agric 22 (2006) 421–426.
[7] Z. Phiri, R.C. Everson, H.W. Neomagus, B.J. Wood, BJ. The effect of acid demineralising bituminous coals and de-ashing the respective chars on nitrogen functional forms. J. Anal. Appl. Pyrol.., 125, pp.127–135.
[8] R.C. Uwaoma, C.A. Strydom, R.H. Matjie, Bunt J.R, Influence of density separation of selected South African coal fines on the products obtained during liquefaction using tetralin as a solvent, Energ. Fuel. 33 (2019) 1837–1849.
[9] K.N. Finney, V.N. Sharifi, J. Swithenbank, Fuel palletisation with a binder: part I - Identification of a suitable binder for spent mushroom compost-coal tailing pellets, Energ. Fuel. 23 (2009) 3195–3202.
[10] M.C.F. Toledo, P.M. Kuznesof, Calcium lignosulfonate chemical and technical assessment, in: Proceedings of the Joint FAO/WHO Expert Committee on Food Additives 69, 2008, pp. 1–8.
[11] R. Guan, W. Li, B. Li, Effects of Ca-based additives on desulfurisation during coal pyrolysis, Fuel 82 (2003) 1961–1966.
[12] P.L. Walker, Catalysis of lignite char gasification by exchangeable calcium and magnesium, Fuel 63 (1984) 1214–1220.
[13] C. Shuai, S. Hu, L. He, J. Xiang, L. Sun, S. Su, L. Jiang, Q. Chen, C. Xu, The synergistic effect of Ca (OH)2 on the process of lignite steam gasification to produce hydrogen-rich gas, Int. J. Hydrog. Energy 39 (2014) 15506–15516.
[14] K. Murakami, M. Sato, N. Tsubouchi, Y. Ohtsuka, K. Sugawara, Steam gasification of Indonesian sub-bituminous coal with calcium carbonate as a catalyst raw material, Fuel Process. Technol. 129 (2015) 91–97.
[15] R.C. Uwaoma, C.A. Strydom, Matjie R.H, J.R. Bunt, Gasification of chars from tetralin liquefaction of< 1.5 g cm−3 carbon-rich residues derived from waste coal fines in South Africa, J. Therm. Anal. Calorim. (2021) 1–15.
[16] P.C. Koenig, R.G. Squires, N.M. Laurendeau, Char gasification by carbon dioxide: further evidence for a two-site model, Fuel 65 (1986) 412–416.
[17] C.A. Strydom, A.C. Collins, J.R. Bunt, The influence of various potassium compound additions on the plasticity of a high-swelling South African coal under pyrolysing conditions, J. Anal. Appl. Pyrol. 112 (2015) 221–229.
[18] Y. Önal, K. Ceylan, Effects of treatments on the mineral matter and acidic functional group contents of Turkish lignites, Fuel 74 (1995) 972–977.
[19] N. Wijaya, L. Zhang, A critical review of coal demineralisation and its implication on understanding the speciation of organically bound metals and submicrometer mineral grains in coal, Energ. Fuel. 25 (2011) 1–16.
[20] X.G. Li, B.G. Ma, L. Xu, Z.W. Hu, X.G. Wang, Thermogravimetric analysis of the co-combustion of the blends with high ash coal and waste tyres, Thermochim. Acta. 441 (2006) 79–83.
[21] J. Cheng, J.H. Zhou, J.Z. Liu, Z.J. Zhou, X.Y. Cao, K.F. Cen, Effect of Carbide Line on Various Coal Combustion, J. Fuel Chem. Technol. 32 (2004) 37–42.
[22] X.G. Li, Y. Lv, B.G. Ma, S.W. Jian, H.B. Tan, Thermogravimetric investigation on co-combustion characteristics of tobacco residue and high-ash anthracite coal, Bioresour. Technol. 102 (2011) 9783–9787.
[23] H.M. Rietveld, A profile refinement method for nuclear and magnetic structures, J. Appl. Crystallogr. 2 (1969) 65–71.
[24] S.A. Speakman, Introduction to PANalytical X'Pert HighScore Plus v3. 0, MIT Center Mater. Sci. Eng. (2012) 1–19.
[25] K. Norrish, J.T. Hutton, An accurate X-ray spectrographic method for the analysis of a wide range of geological samples, Geochim. Cosmochim. Acta 33 (1969) 431–453.
[26] R.H. Matjie, Z. Li, C.R. Ward, J. Kosasi, J.R. Bunt, J.C.A. Strydom, Mineralogy of furnace deposits produced by South African coals during pulverised-fuel combustion tests, Energ. Fuel. 29 (2015) 8226–8238.
[27] W.B. Li, J.D. Lu, M.R. Dong, S.Z. Lu, J.H. Yu, S.S. Li, J.W. Huang, J. Liu, Quantitative analysis of calorific value of coal-based on spectral preprocessing by laser-induced breakdown spectroscopy (LIBS) Energ, Fuel 32 (2018) 24–32.
[28] R.H. Matjie, J.M. Lesufi, J.R. Bunt, C.A. Strydom, H.H. Schobert, R.C. Uwaoma, In situ capturing and absorption of sulfur gases formed during thermal treatment of South African coals, ACS Omega 3 (2018) 14201–14212.
[29] H. Shirai, M. Ikeda, H. Aramaki, Characteristics of hydrogen sulfide formation in pulverised coal combustion, Fuel 114 (2013) 114–119.
[30] Z. Ma, J. Bai, W. Li, Z. Bai, L. Kong, Mineral transformation in char and its effect on coal char gasification reactivity at high temperatures, Part 1: mineral transformation in char, Energ. Fuel. 27 (2013) 4545–4554.
[31] X. Yan, D. Che, Xu T, Effect of rank, temperatures and inherent minerals on nitrogen emissions during coal pyrolysis in a fixed bed reactor, Fuel Process. Technol. 86 (2005) 739–756.
[32] Q. Liu, H. Hu, Q. Zhou, S. Zhu, G. Chen, Effect of inorganic matter on reactivity and kinetics of coal pyrolysis, Fuel 83 (2004) 713–718.
[33] N.A. Öztaş, Y. Yürüm, Pyrolysis of Turkish Zonguldak bituminous coal. Part 1. Effect of mineral matter, Fuel 79 (2000) 1221–1227.
[34] M. Rahman, A. Samanta, R. Gupta, Production and characterisation of ash-free coal from low-rank Canadian coal by solvent extraction, Fuel Process. Technol. 115 (2013) 88–98.
[35] B. Xiao, X. Sun, Chemical, structural, and thermal characterisations of alkali-soluble lignins and hemicelluloses, and cellulose from maise stems, rye straw, and rice straw, Polym. Degrad. Stab. 74 (2001) 307–319.
[36] E. Jakab, O. Faix, F. Till, T. Székely, Thermogravimetry/mass spectrometry study of six lignins within the scope of an international round robin test, J. Anal. Appl. Pyrol. 35 (1995) 167–179.
[37] S. Liodakis, G. Katsigiannis, G. Kakali, Ash properties of some dominant Greek forest species, Thermochim. Acta. 437 (2005) 158–167.
[38] P.L. Walker Jr, F. Rusinko Jr, L.G. Austin, Gas reactions of carbon, Adv. Catal. 11 (1959) 133–221.
[39] P. Lahijani, Z.A. Zainal, A.R. Mohamed, M. Mohammadi, Co-gasification of tire and biomass for enhancement of tire-char reactivity in CO2 gasification process, Bioresour. Technol. 138 (2013) 124–130.
[40] W. Huo, Z. Zhou, X. Chen, Z. Dai, G. Yu, Study on CO2 gasification reactivity and physical characteristics of biomass, petroleum coke and coal chars, Bioresour. Technol. 159 (2014) 143–149.
[41] Y. Zhang, M. Ashizawa, S. Kajitani, K. Miura, Proposal of a semi-empirical kinetic model to reconcile with gasification reactivity profiles of biomass chars, Fuel 87 (2008) 475–481.